

## The role of relative humidity in continental new particle formation

Amar Hamed,<sup>1</sup> Hannele Korhonen,<sup>1,2</sup> Sanna-Liisa Sihto,<sup>3</sup> Jorma Joutsensaari,<sup>1</sup> Heikki Järvinen,<sup>4</sup> Tuukka Petäjä,<sup>3</sup> Frank Arnold,<sup>5</sup> Tuomo Nieminen,<sup>3</sup> Markku Kulmala,<sup>3</sup> James N. Smith,<sup>1,6,7</sup> Kari E. J. Lehtinen,<sup>1,6</sup> and Ari Laaksonen<sup>1,8</sup>

Received 12 March 2010; revised 20 September 2010; accepted 29 October 2010; published 1 February 2011.

[1] Relative humidity (RH) has been observed to be anticorrelated with continental new particle formation. Several reasons have been proposed for this rather surprising finding, but no firm conclusions have been drawn so far. Here we study several of the proposed reasons: Enhanced coagulative scavenging of sub-3 nm clusters at high RH, diminished solar radiation at high RH leading to diminished gas phase oxidation chemistry, and increased condensation sink (CS) of condensable gases due to hygroscopic growth of the preexisting particles. Our theoretical calculations indicate that the increase of coagulative scavenging plays a relatively small role in the inhibition of nucleation at high RH. On the other hand, field data show that the maximum observed gas phase sulphuric acid concentrations are limited to RHs below 60%. The field data also indicate that this is likely due to low OH concentrations at high RH. This finding is also supported by aerosol dynamics model simulations. The model was used to find out whether this is mainly due to decreased source (solar radiation) or increased sink (CS) terms at the elevated RH. The simulation results show that the decreased source term at high RH limits H<sub>2</sub>SO<sub>4</sub> levels in the air, and therefore high new particle formation rates (above ~1 cm<sup>-3</sup> s<sup>-1</sup>) rarely occur above 80% RH.

**Citation:** Hamed, A., et al. (2011), The role of relative humidity in continental new particle formation, *J. Geophys. Res.*, 116, D03202, doi:10.1029/2010JD014186.

### 1. Introduction

[2] It has been observed at different continental locations that new particle formation (NPF) takes place preferentially at low relative humidities (RH) [e.g., *Birmili and Wiedensohler*, 2000; *Woo et al.*, 2001; *Boy and Kulmala*, 2002; *Alam et al.*, 2003; *Birmili et al.*, 2003; *Stanier et al.*, 2004; *Hyvönen et al.*, 2005; *Mikkonen et al.*, 2006; *Hamed et al.*, 2007; *Laaksonen et al.*, 2008; *Jaatinen et al.*, 2009; *Vaattovaara et al.*, 2009]. Furthermore, observations show that during NPF events, there is an anticorrelation between RH and formation rate [*Sihto et al.*, 2006] or between RH and the number concentration [*Weber et al.*, 1997; *Jeong et al.*, 2004] of freshly formed particles. These findings are somewhat surprising as the main species responsible for atmospheric nucleation and early particle growth is thought to be sulphuric acid (H<sub>2</sub>SO<sub>4</sub>) which is

known to nucleate very efficiently with water vapor so that, in laboratory experiments, nucleation rates increase with RH at fixed sulfuric acid concentration and no background aerosol. Of course, some other species such as ammonia and organics might also be involved in atmospheric NPF. Also, a number of observations have been made on NPF in the vicinity of clouds [e.g., *Hegg et al.*, 1990; *Clarke et al.*, 1998; *Keil et al.*, 2001], where the RH is very high, usually over 90%.

[3] A number of reasons have been suggested as to why high RH could possibly suppress NPF. Preexisting aerosol particles take up water vapor as RH increases, which causes both the condensation and the coagulation sinks to increase. An increased condensation sink (CS) means a larger loss term for condensable vapors such as H<sub>2</sub>SO<sub>4</sub> which might contribute to the anticorrelation between the NPF rate and RH and, in extreme cases, even inhibit nucleation. An increased coagulation sink (CoagS) causes increased coagulative scavenging of freshly formed nuclei onto the preexisting particles before the nuclei have grown large enough to be detected by aerosol instruments. This could cause an apparent anticorrelation between the NPF rate and RH; however, the anticorrelation remains even after accounting mathematically for the effect of (RH-dependent) CoagS on nucleation rate [see *Sihto et al.*, 2006]. On the other hand, increased CoagS might “mask” nucleation events in some cases by removing virtually all nuclei before they are detected.

[4] Another possible reason for the observed negative correlations between RH and NPF is that solar radiation, which

<sup>1</sup>Department of Physics and Mathematics, University of Eastern Finland, Kuopio, Finland.

<sup>2</sup>Now at Finnish Meteorological Institute, Kuopio, Finland.

<sup>3</sup>Department of Physics, University of Helsinki, Helsinki, Finland.

<sup>4</sup>Finnish Meteorological Institute, Helsinki, Finland.

<sup>5</sup>Atmospheric Physics Division, Max-Planck Institute for Nuclear Physics, Heidelberg, Germany.

<sup>6</sup>Also at Finnish Meteorological Institute, Kuopio, Finland.

<sup>7</sup>Also at Atmospheric Chemistry Division, National Center for Atmospheric Research, Boulder, Colorado, USA.

<sup>8</sup>Also at Finnish Meteorological Institute, Helsinki, Finland.

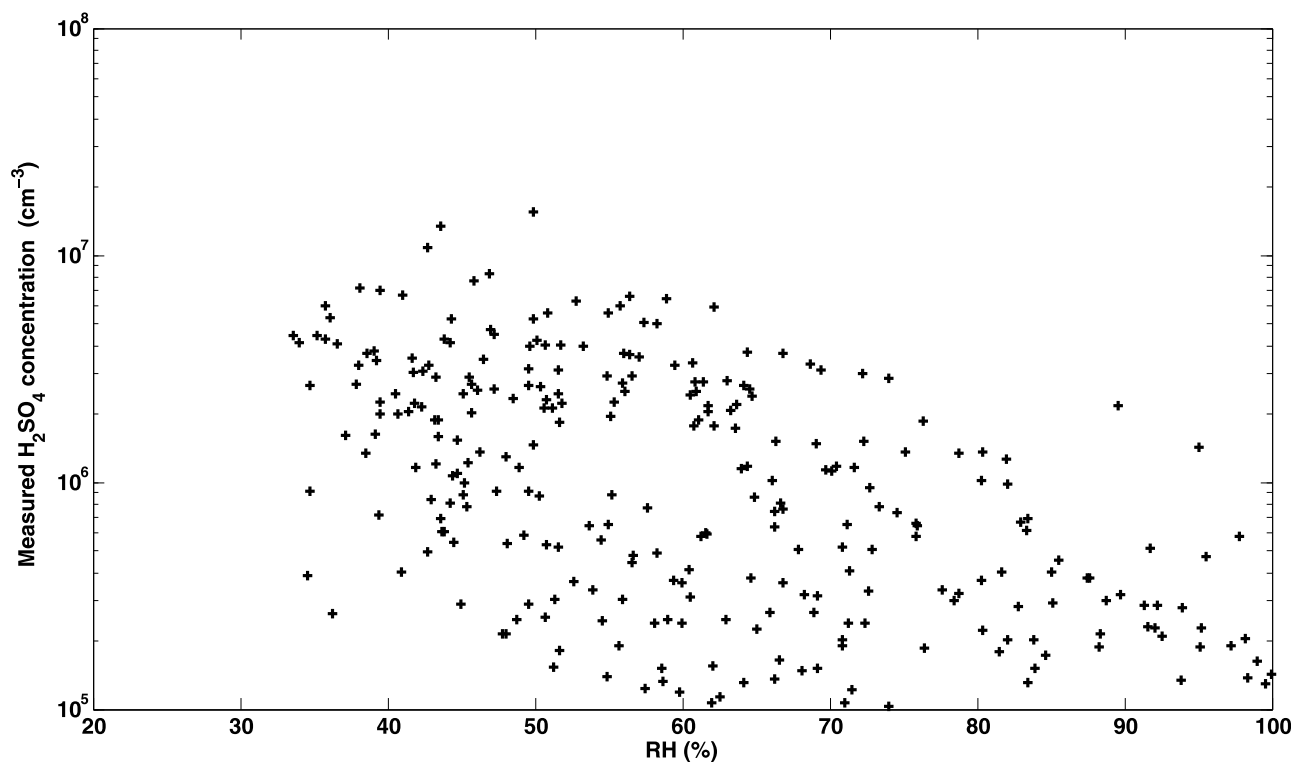


**Figure 1.** RH (%) versus  $\text{H}_2\text{SO}_4$  concentrations ( $\text{cm}^{-3}$ ) observed during the 2003 QUEST field campaign in Hyytiälä, Finland. Data points represent 1 h averages from 0600 to 1800 LT.

drives the photochemistry leading to formation of  $\text{H}_2\text{SO}_4$  and condensable organics, is often less intense at high RH, either because of cloudiness or for the simple reason that diurnal RH behavior is often such that there is a minimum at around noon when NPF events are frequently observed. Still other reasons have been presented [e.g., *Hyvönen et al.*, 2005; *Bonn et al.*, 2002; *Bonn and Moortgat*, 2003], that suggest that low volatility ozonolysis products of monoterpenes and sesquiterpenes, whose formation is known to be suppressed by water vapor, might be involved in atmospheric nucleation and subsequent growth. Note however, that in this case it is not the RH but the absolute humidity which would cause the anticorrelation with NPF. Although absolute humidity has also been noted to anticorrelate with NPF [e.g., *Boy and Kulmala*, 2002; *Komppula et al.*, 2003; *Lyubovtseva et al.*, 2005; *Hamed et al.*, 2007], we will in this paper mostly focus on the role of RH.

[5] The aim of this study is to find out whether increased CS, increased CoagS, or decreased radiation suppresses NPF in humid conditions. In order to achieve this goal, we examine the above suggested possibilities in more detail, using analysis of field measurements, theoretical calculations, and aerosol dynamics model simulations.

## 2. Analysis of Field Measurements From QUEST 2003 Campaign

### 2.1. Brief Description of Measurements and Collected Data

[6] Particle size distributions have been measured continuously at the Station for Measuring Ecosystem-Atmosphere Relations (SMEAR) at the Hyytiälä forestry station

(SMEAR II;  $61^{\circ}51'\text{N}$ ,  $24^{\circ}17'\text{E}$ ; 170 m above sea level), southern Finland since January 1996 [*Hari and Kulmala*, 2005]. The measurements are carried out using a twin Differential Mobility Particle Sizer (DMPS) system; the first DMPS measures particle size distributions between 3 and 20 nm and the second one between 15 and 600 nm. One measurement cycle lasts for 10 min (more detail is given by *Aalto et al.* [2001]). In addition to particle size distribution measurements, several gas and meteorological parameters are measured at the SMEAR II station (e.g.,  $\text{SO}_2$ , NO,  $\text{NO}_2$ ,  $\text{NO}_x$ , CO,  $\text{CO}_2$ ,  $\text{H}_2\text{O}$ ,  $\text{O}_3$ , temperature, relative humidity, wind direction, wind speed, global radiation, precipitation, and atmospheric pressure).

[7] The Quantification of Aerosol Nucleation in the European Boundary Layer (QUEST) field campaign at the SMEAR II station took place from 18 March to 9 April 2003 [*Sihto et al.*, 2006]. The QUEST 2003 data set is unique in the sense that during the campaign a large number of events were observed (from a total of 23 measurement days, 20 were NPF days that we have used in our study). During this spring campaign, the gas phase sulphuric acid concentration was measured by a chemical ionization mass spectrometer (CIMS) [*Hanke et al.*, 2002]. The time resolution of the spectrometer was less than 1 s, but the data was averaged over 60 s in order to reduce statistical error and sampling noise. The sulphuric acid detection limit was  $1 \times 10^5 \text{ cm}^{-3}$  and the relative measurement uncertainty 30%. In our analysis of NPF days we make use of the particle size distribution data together with RH, absolute humidity, UV radiation, and  $\text{SO}_2$  concentrations from this campaign period. As nucleation mostly takes place during

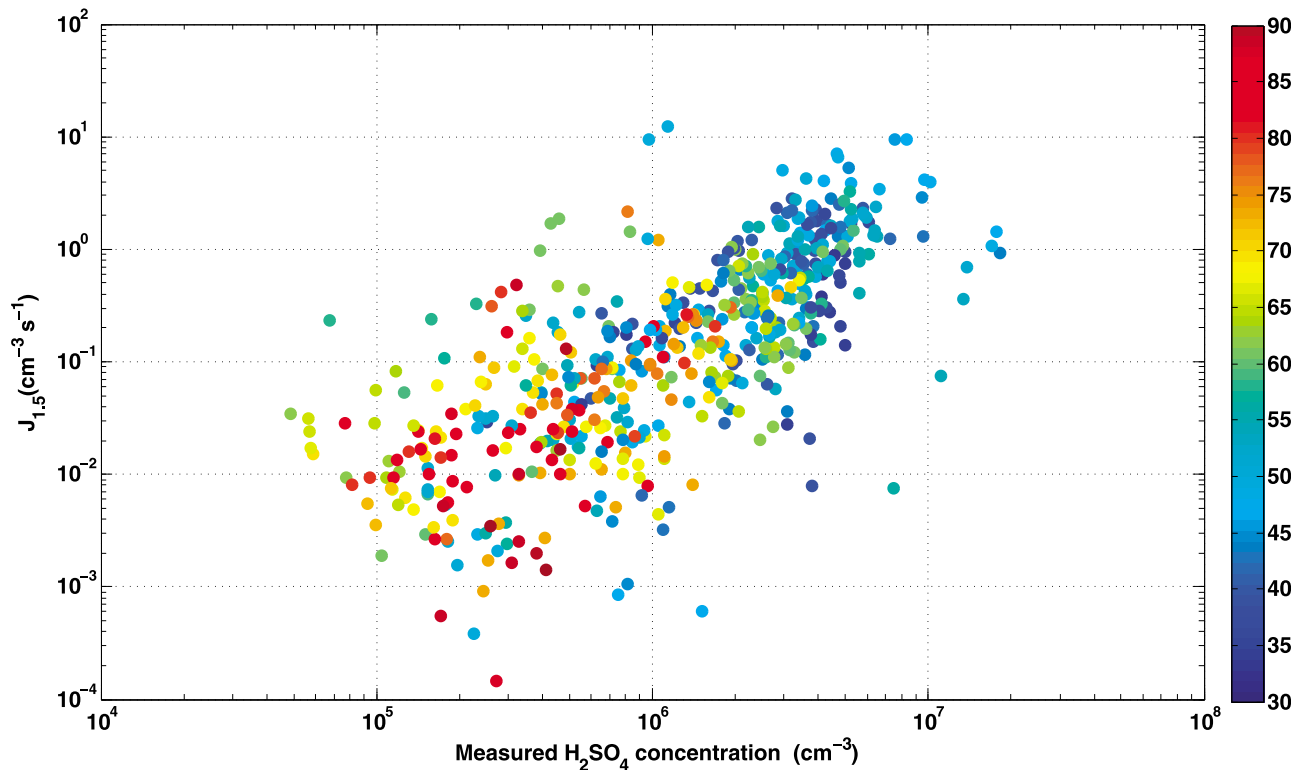


**Figure 2.** Nucleation rate at 1.5 nm ( $J_{1.5}$ ) versus  $[\text{H}_2\text{SO}_4]$  measured during the 2003 QUEST campaign in Hyytiälä, Finland. Color coding indicates relative humidity (RH) expressed as percent. Data points represent 10 min averages from 0600 to 1800 LT.

daylight hours, we limit our analysis to 0600–1800 local time (LT).

[8] The nucleation rate of critical clusters of 1.5 nm in diameter ( $J_{1.5}$ ) is a central quantity in this analysis. The  $J_{1.5}$  rate was extrapolated from the formation rate of 3 nm particles,  $J_3$ , which is obtained from measured particle size distributions. Particularly, we apply the method presented by *Lehtinen et al.* [2007] (see equation (1)). The growth rate (GR in  $\text{nm h}^{-1}$ ) is estimated by incorporating the probability that a particle would grow from 1 to 3 nm by vapor condensation before being scavenged by the preexisting aerosol. Time delay  $dt$  in equation (1) is estimated for each NPF day as the delay between the rise in sulfuric acid concentrations and particle number concentration for particles between 3 and 6 nm ( $N_{3-6}$ ). The NPF event is assumed to begin when  $[\text{H}_2\text{SO}_4]$  begins to rise sharply, and  $N_{3-6}$  particle concentrations begin to increase as well. In this study, time delay values between rise of  $[\text{H}_2\text{SO}_4]$  and  $N_{3-6}$  varied between 20 min and 1.5 h for different NPF days. For more detailed information about the calculation of nucleation rates, see, for example, *Kerminen and Kulmala* [2002], *Sihto et al.* [2006], and *Lehtinen et al.* [2007].

## 2.2. Effect of Relative Humidity on $\text{H}_2\text{SO}_4$ Concentrations and Nucleation Rates ( $J_{1.5}$ )

[9] We will first look at how the measured sulphuric acid concentrations behave at different relative humidities. Sulphuric acid is currently thought to be the most likely nucleation precursor candidate as well as to contribute to the growth of newly formed particles [*Weber et al.*, 1999; *Kulmala*, 2003;

*Kulmala et al.*, 2004a; *Sipilä et al.*, 2010]. Therefore variations in its concentration as a function of RH should directly affect both nucleation (taking place at  $\sim 1\text{--}1.5$  nm) and NPF (at  $\sim 3$  nm) rates. Measurements during the 2003 QUEST field campaign show a clear RH dependence of the gas phase  $\text{H}_2\text{SO}_4$  concentrations with decreasing values at RH above  $\sim 60\%$  (Figure 1). Figure 1 shows that the decrease of the maximum concentrations is about an order of magnitude or even more between 60 and 90% RH. The RH effect is also seen in the calculated nucleation rates. Figure 2 shows a scatterplot of  $J_{1.5}$  calculated from the measured aerosol size distributions versus measured  $[\text{H}_2\text{SO}_4]$ . The data points are color-coded according to RH. As Figure 2 shows, at high RH ( $>80\%$ ) the  $\text{H}_2\text{SO}_4$  concentrations are below  $3 \times 10^6 \text{ cm}^{-3}$  and the nucleation rates are mostly below  $2 \text{ cm}^{-3} \text{ s}^{-1}$ .

[10] Taken together Figures 1 and 2 strongly suggest that the suppression of nucleation at humid conditions is linked to either the formation or the loss rate of sulphuric acid. We will investigate both of these possibilities below.

## 2.3. Effect of RH on $\text{SO}_2$ and OH Concentrations

[11] High RH can, in principle, affect the atmospheric concentrations of both  $\text{SO}_2$  and OH. At high RH the amount of liquid water available in the atmosphere (associated either with hygroscopic aerosol particles or clouds) increases, which could lead to more efficient aqueous phase conversion of  $\text{SO}_2$  to sulfate, and thus to decreased gas phase  $\text{SO}_2$  concentrations. However, measurements of  $\text{SO}_2$  during the QUEST 2003 campaign do not support any significant RH dependence (Figure 3a). In Figure 3a we highlight (diamonds)

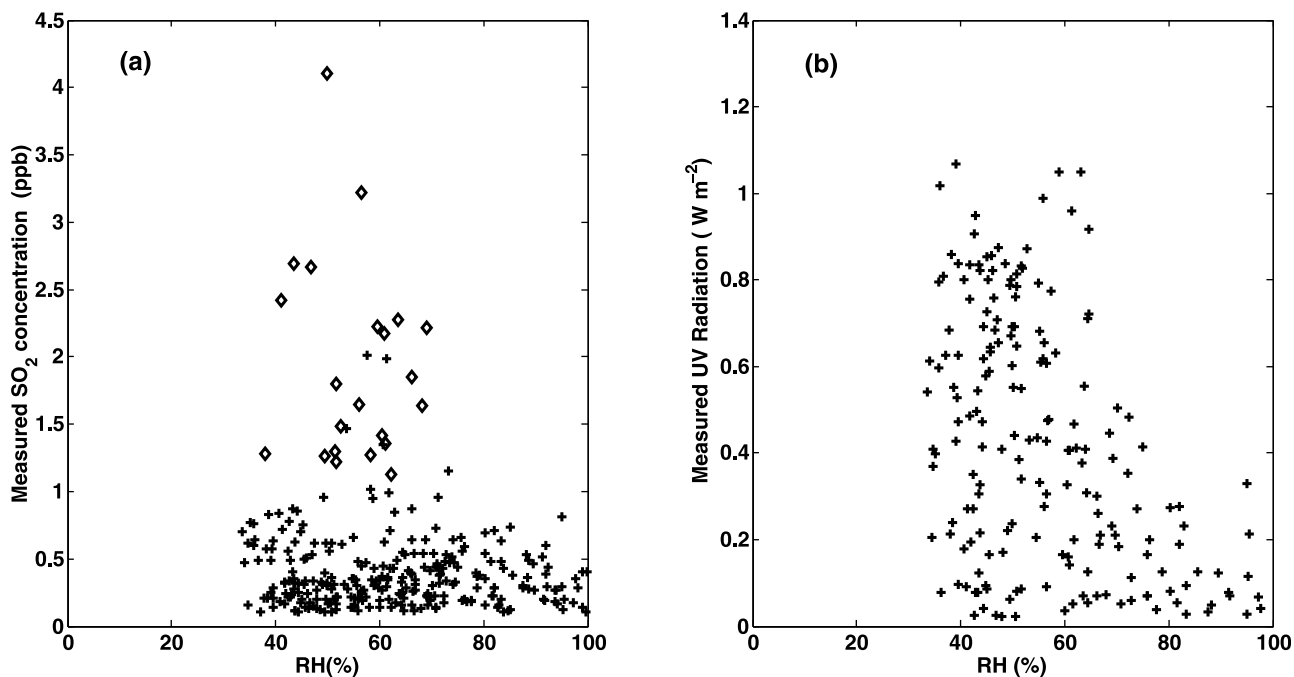


**Figure 3.** RH (%) versus (a)  $\text{SO}_2$  concentrations (ppb) (the high  $\text{SO}_2$  concentrations on 1 and 2 April 2003 are indicated by diamonds) and (b) UV radiation in  $\text{W m}^{-2}$  observed during the 2003 QUEST campaign in Hyttiälä, Finland. Data points represent 1 h averages from 0600 to 1800 LT.

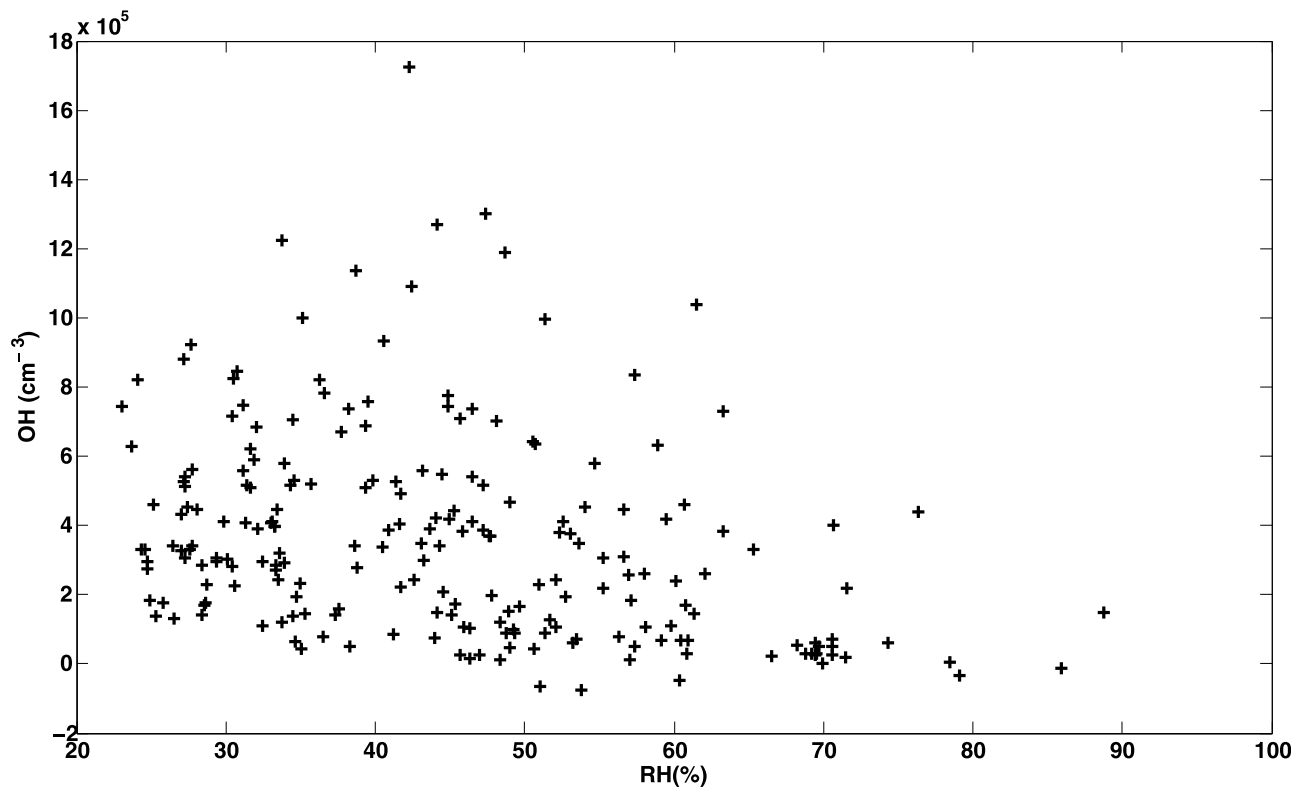


**Figure 4.** RH (%) versus OH concentrations in  $\text{cm}^{-3}$  units observed during a 2007 field campaign in Hyttiälä, Finland. Data points represent 1 h averages from 0600 to 1800 LT.

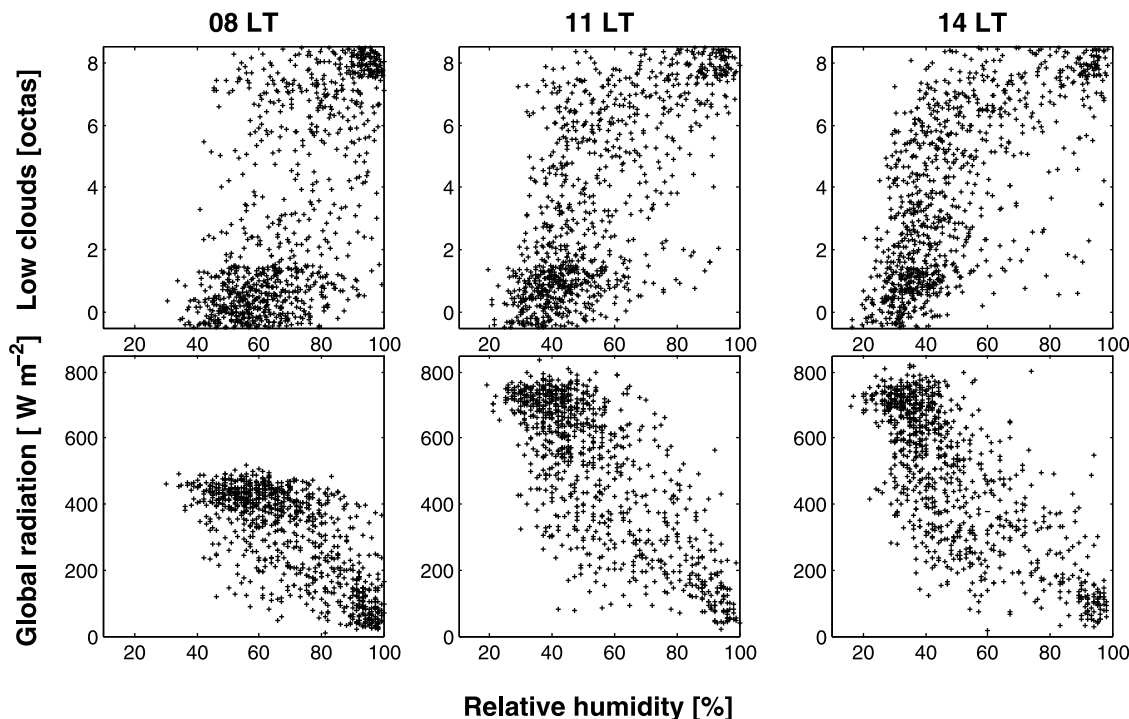


**Figure 5.** A 30 year data set (1970–2000) of (top) low-level cloudiness (octa units, where an octa is a cloudiness fraction given as a score of 1–8 (e.g., 3 octas indicates three eighths cloudiness)) and (bottom) global radiation ( $\text{W}/\text{m}^2$ ) versus relative humidity (%) at the Finnish Meteorological Institute’s observatory in Jokioinen ( $60^\circ 49' \text{N}$ ,  $23^\circ 30' \text{E}$ ), southern Finland. The data shown are for (left) 0800, (middle) 1100, and (right) 1400 LT.

measurements from two days (1 and 2 April) in which polluted air impacted this remote site. These points are considered outliers, since the preponderance of  $\text{SO}_2$  concentrations in the 40–70% RH range fall below 0.5 ppb (the average and median  $\text{SO}_2$  concentration over this range of RH are 0.5 and 0.3 ppb, respectively). A similar analysis of longer, multiyear data sets (not shown) from Hyytiälä, Finland and San Pietro Capofiume, Italy support the observations shown in Figure 3a that  $\text{SO}_2$  concentrations are not correlated with RH.

[12] Recent studies have suggested that the tropospheric OH radical concentration is strongly correlated with the intensity of solar UV radiation despite the complex OH chemistry in the atmosphere [Rohrer and Berresheim, 2006; Petäjä *et al.*, 2009]. Since direct measurements of OH concentrations were not made during QUEST, we use the measurements of UV as a proxy for OH. The highest UV radiation values during this campaign are limited to RH values of  $\sim 60\%$  and, at higher humidities, the maximum values decrease steeply (Figure 3b). This trend is very similar to that of the measured  $\text{H}_2\text{SO}_4$  concentrations (Figure 1) giving indications that the sulfuric acid concentration at high humidities is controlled by the reduced OH concentrations. One additional piece of evidence supports the hypothesis that reductions in sulphuric acid may be related to reduced OH levels comes from the recent European Integrated project on Aerosol Cloud Climate and Air Quality Interactions (EUCAARI) campaign [Petäjä *et al.*, 2009], during which OH concentration measurements were made. Figure 4 shows a plot of [OH] versus RH from that campaign. Qualitatively, the OH levels during the 2007 campaign display the same trends as

sulfuric acid (Figure 1) and UV (Figure 3b). Thus a picture emerges from the consistent measurements made at Hyytiälä, that OH levels may play a key role in the observed dependence of new particle formation on RH.

[13] There are two reasons for the RH dependence of OH concentrations that act simultaneously. First, solar radiation is attenuated on cloudy and hazy days. This is seen in a climatological data set from the Jokioinen observatory ( $\sim 100$  km from Hyytiälä station) which shows that the low-level cloud cover correlates with the ground level RH (Figure 5, top). Thus as a result of cloudiness, global solar radiation anticorrelates with RH and global radiation reaching the ground level is reduced at RH greater than  $\sim 60\%$  (Figure 5, bottom). On the other hand, it is well known from the over 10 years of measurements from Hyytiälä that NPF does not occur on cloudy days with low radiation [Boy and Kulmala, 2002; Dal Maso *et al.*, 2005].

[14] Second, RH and solar radiation typically show clear diurnal cycles that are opposite in phase. In the morning, as sunlight warms the ground layer, RH often starts to decrease, and will increase again at noon and toward sunset. Hence, there is an anticorrelation between RH and solar radiation. On annual time scales this anticorrelation may be smeared as the daily peak intensity of the radiation varies strongly from midwinter to midsummer, but on monthly time scales it should be detectable. On NPF days (which are in general rather sunny) the opposite diurnal cycles of RH and radiation is the most likely explanation for their anticorrelation, although cloudiness may play a minor role.

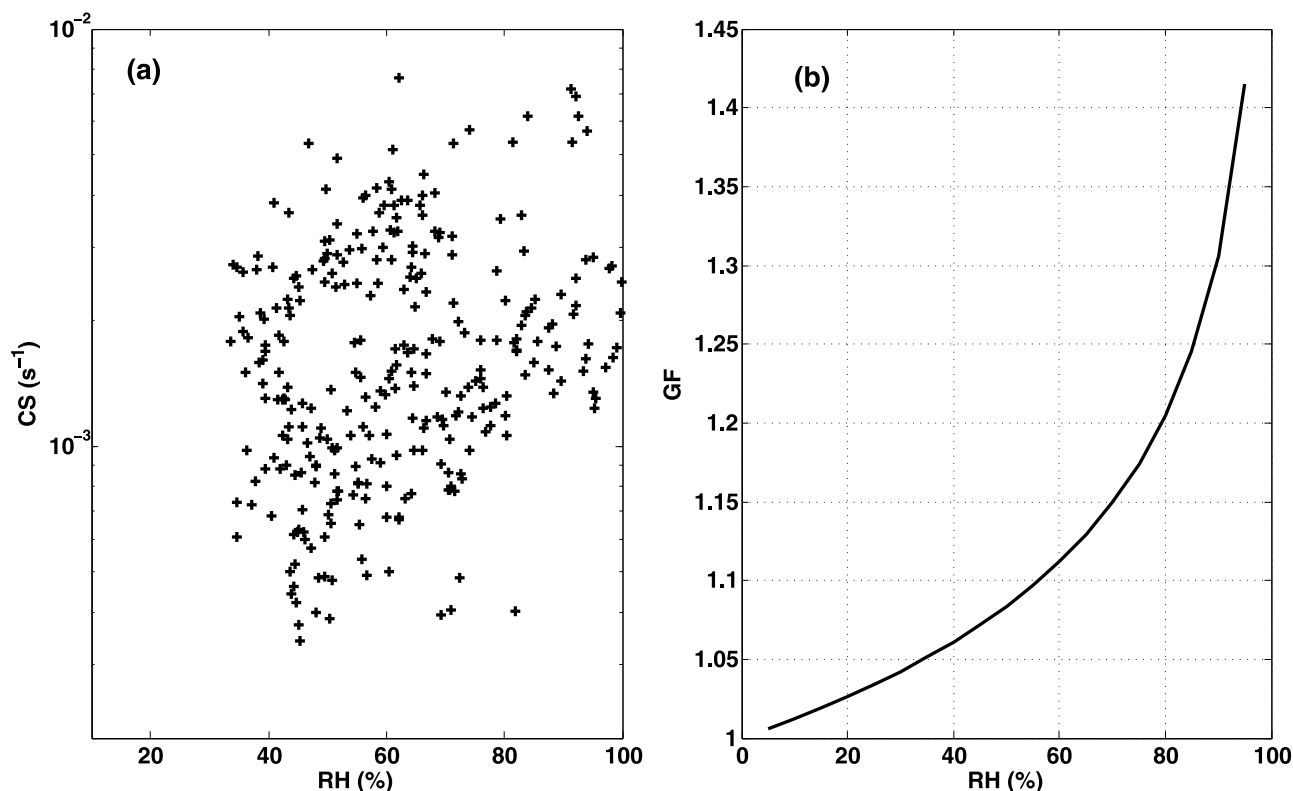


**Figure 6.** (a) RH (%) versus condensation sink ( $CS, s^{-1}$ ) estimated during the 2003 QUEST field campaign in Hyytiälä, Finland. (b) The hygroscopic growth factor (GF) of dry 100 nm particles as a function of RH using Laakso *et al.*'s [2004] formula.

[15] It is also noteworthy that the OH concentration is very likely to affect the formation rate of low volatility and semivolatile organic compounds from plant emitted VOCs. Thus lower OH at high RH may affect the observed nucleation rates also via reduced new particle growth rates due to the lower concentrations of condensable organic materials.

#### 2.4. Effect of RH on Condensation Sink

[16] The size of aerosol particles, and thus the sink for condensable vapors, grows very efficiently as a function of RH. Figure 6 shows the estimated condensation sink (CS) values as a function of RH measured during the 2003 QUEST campaign (note that the CS values have been calculated from dry size distributions using the method described by Pirjola *et al.* [1998] and by applying an RH correction using Laakso *et al.*'s [2004] parameterization); between 30 and 90% RH, the value of CS increases roughly by a factor of 3.

#### 2.5. Effect of Other Atmospheric Variables

[17] Boy and Kulmala [2002] found that on NPF event days, the water vapor concentration (absolute humidity) is generally lower than on nonevent days of the corresponding month. One reason why high absolute humidity could affect NPF events is that water vapor inhibits certain reactions in the ozonolysis of VOCs and thus prevents the formation of condensable organics to some extent. We therefore made a plot similar to that shown in Figure 2, but color scaled according to absolute rather than relative humidity (Figure 7).

It can be seen that, unlike RH, the high and low absolute humidity values are rather evenly spread within the data set, and thus reveals no absolute humidity effect on the NPF.

### 3. Theoretical Analysis of the Effect of Coagulation Sink (CoagS)

[18] The effect of an increased coagulation sink on NPF rates at high humidities is difficult to evaluate directly from field measurements. Therefore, we investigate its role theoretically, and make calculations based on observed variables affecting coagulation scavenging of freshly formed nuclei. In this section we focus on considering the possibility that the increase of CoagS at increased RH causes masking of NPF events (i.e., nucleation occurs at 1.5 nm, but because of the increased sink, such a large fraction of the freshly formed particles is scavenged by coagulation before reaching 3 nm that the event cannot be observed).

#### 3.1. Background

[19] Atmospheric NPF is usually observed with instruments capable of detecting particles larger than about 3 nm in diameter (although in very recent instruments the detection limit has been lowered to  $\sim 2$  nm [see Kulmala *et al.*, 2007; Iida *et al.*, 2009]). Therefore, the actual freshly nucleated particles, with diameters closer to 1 nm [McMurry and Friedlander, 1979; Kulmala, 2003] are not directly observed. The current view of atmospheric NPF is as follows: (1) Sulphuric acid and/or some other sulphur species,

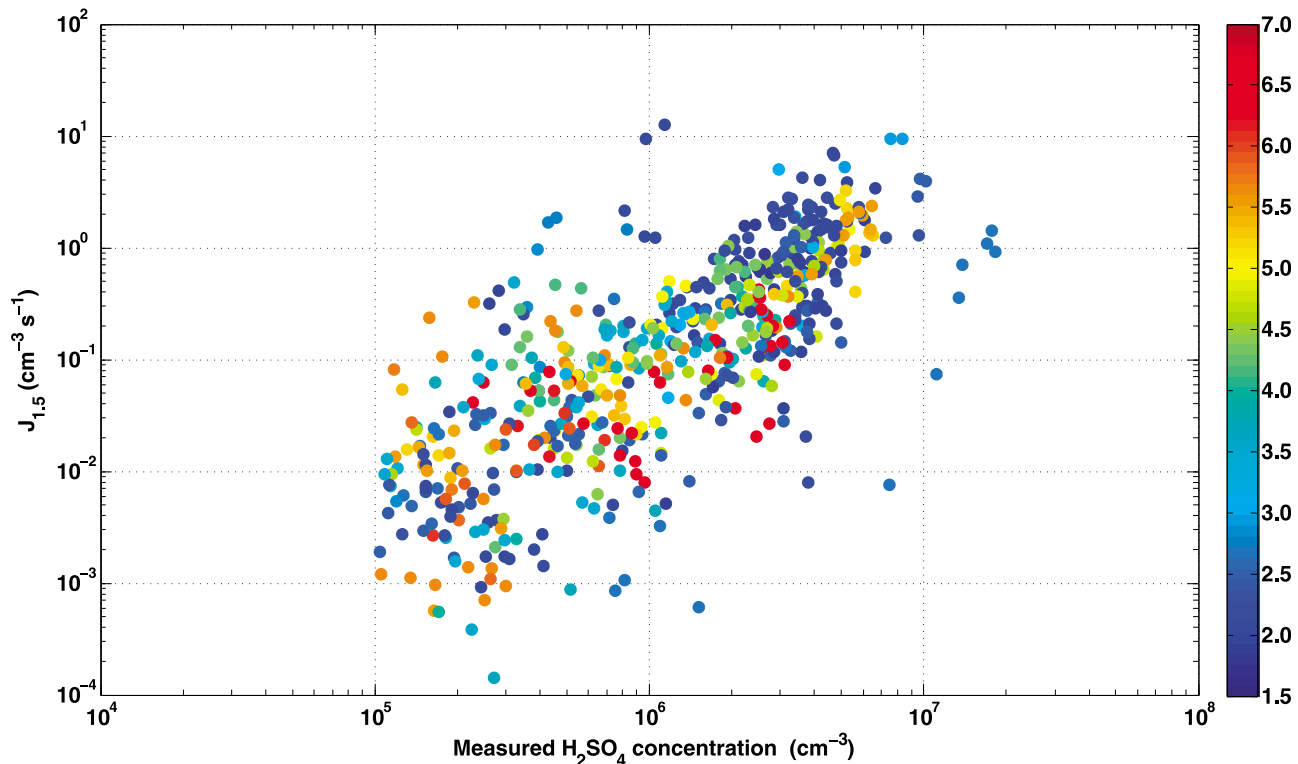


**Figure 7.** Nucleation rate at 1.5 nm ( $J_{1.5}$ ) versus  $[\text{H}_2\text{SO}_4]$  measured during the 2003 QUEST field campaign in Hyytiälä, Finland. Color coding indicates absolute humidity. Data points represent 10 min averages from 0600 to 1800 LT.

together with some other molecules such as water, ammonia, or some organics, produce stable critical nuclei at a 1 nm mass diameter, which corresponds to  $\sim 1.5$  nm mobility diameter [Laaksonen *et al.*, 2008; Kulmala *et al.*, 2007]. (2) The critical nuclei start growing by condensation of  $\text{H}_2\text{SO}_4$  or low volatility organic vapor. (3) If condensable organics have not participated in the growth of the nuclei from 1 nm, it is likely that they start speeding up the growth at some later size when the Kelvin effect has decreased sufficiently, that is, with so-called nano-Köhler mechanisms or via heterogeneous nucleation [Kulmala *et al.*, 2004b]. During the growth toward the detection limit of 3 nm, the growing nuclei are scavenged by coagulation with preexisting aerosol particles. The scavenging efficiency decreases with increasing nucleus size. The following equation [Lehtinen *et al.*, 2007] describes the connection between the actual nucleation rate at 1.5 nm ( $J_{1.5}$ ) and the observed new particle formation rate at 3 nm ( $J_3$ ):

$$J_3(t + dt) = J_{1.5}(t) \exp\left(-\gamma \cdot D_{1.5} \frac{\text{CoagS}(D_{1.5})}{GR}\right), \quad (1)$$

where  $\gamma = \frac{1}{m+1} \left[ \left( \left( \frac{D_3}{D_{1.5}} \right)^{m+1} \right) - 1 \right]$  and  $GR$  denotes the observed growth rate of the particles ( $\text{nm h}^{-1}$ ). The exponent  $m$  depends on the preexisting background size distribution and is given by

$$m = \log \left[ \frac{\text{CoagS}(D_3)}{\text{CoagS}(D_{1.5})} \right] / \log \left[ \frac{D_3}{D_{1.5}} \right]. \quad (2)$$

The  $\text{CoagS}(D_3)$  and  $\text{CoagS}(D_{1.5})$  are the coagulation sinks of nuclei with diameter 3 nm and 1.5 nm, respectively, onto the preexisting particles.

[20] As with CS, the response of the ambient aerosol to humidity-induced growth must be considered in the calculation of coagulation sink [Kulmala *et al.*, 2001; Hämeri *et al.*, 2000]. In order to get more realistic sink values, the measured particle number size distributions at dry conditions were converted into the ones at ambient conditions by applying the hygroscopic growth law given by Laakso *et al.* [2004].

### 3.2. Calculations, Results, and Discussion

[21] Here, we discuss theoretically how increases in the coagulation sink at high RH increases the depletion of freshly nucleated particles before they have grown to the observation limit of 3 nm. We make our calculations based on observed variables affecting coagulational scavenging of freshly formed nuclei. We considered two conditions: An average condition (average  $GR$  values of the newly formed particles and average  $\text{CoagS}$ ) and a slow growth condition (average  $\text{CoagS}$  combined with a  $GR$  that corresponds to slowest observed values). We use the revised formulation of the relation between  $J_3$  and  $J_{1.5}$  presented earlier by Kerminen and Kulmala [2002]. The new formula was given by Lehtinen *et al.* [2007], and it has the advantage that coagulation sink is used instead of CS, and thereby no vapor properties enter the equations.

[22] Assuming that the lowest formation rate that can be reliably detected at 3 nm is  $10^{-3} \text{ cm}^{-3} \text{ s}^{-1}$ , and that the real nucleation rate ( $J_{1.5}$ ) is a  $10^{-2} \text{ cm}^{-3} \text{ s}^{-1}$ , then a 90% loss of

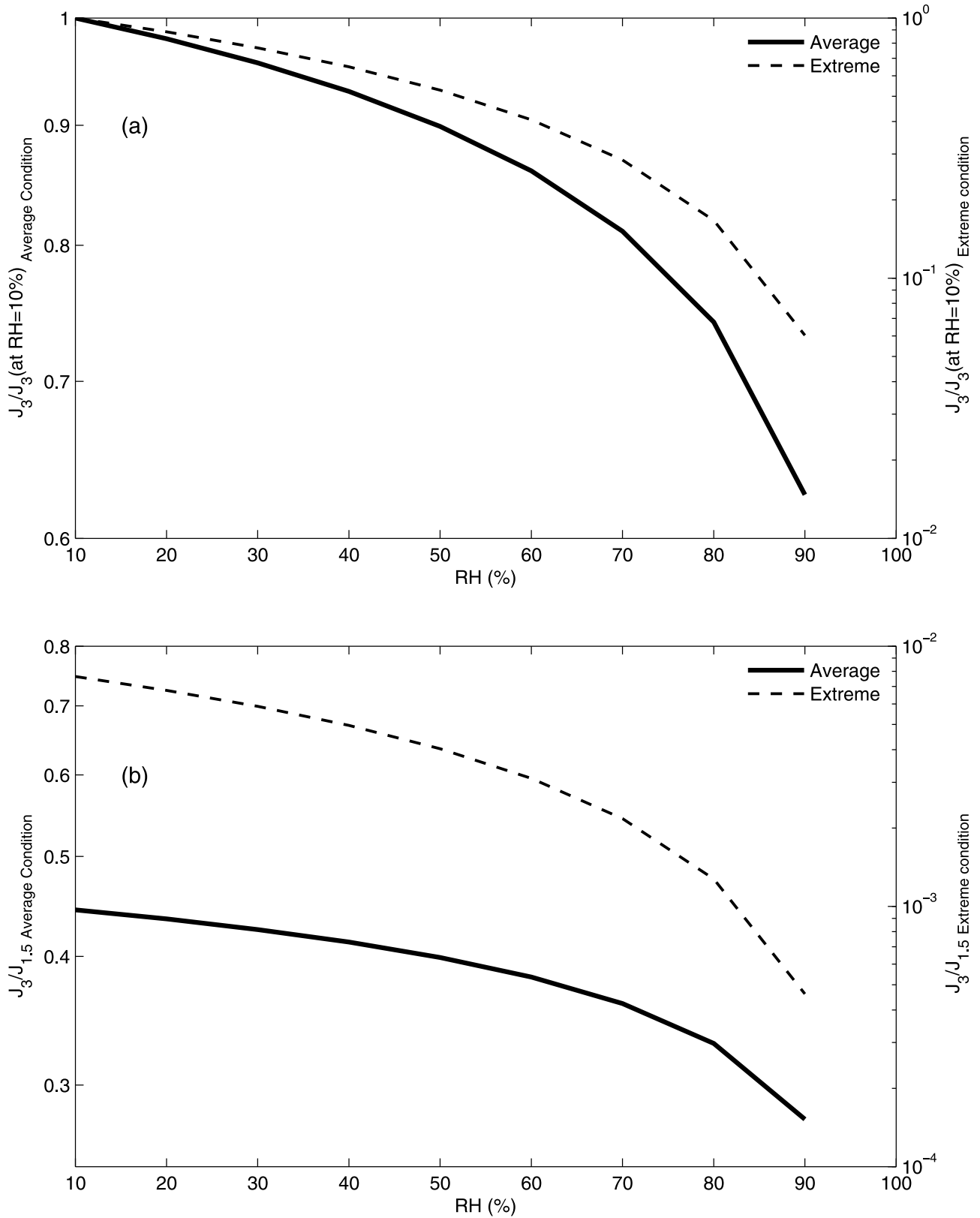


**Figure 8.** (a) Normalized  $J_3$  ( $J_3$  divided by  $J_3$  at 10% RH) and (b)  $J_3/J_{1.5}$  as a function of RH for average (left axis, solid curve) and extreme conditions (right axis, dashed curve). Average conditions correspond to  $GR = 3 \text{ nm h}^{-1}$  and  $CS = 8.6 \text{ h}^{-1}$ , extreme conditions  $GR = 0.5 \text{ nm h}^{-1}$  and  $CS = 8.6 \text{ h}^{-1}$ .



**Table 1.** Parameters Used in Model Simulations

Variable	Values
SO <sub>2</sub> ( $\mu\text{g m}^{-3}$ )	0.5, 5, 50
Organic vapor ( $\text{cm}^{-3}$ )	$10^7$ , $10^8$ , $10^9$
Preexisting particle number ( $\text{cm}^{-3}$ )	50, 500, 5000
<i>A</i> factor ( $\text{s}^{-1}$ )	2E-7, 2E-6, 2E-5

the freshly formed particles by coagulation while they are growing from 1.5 to 3 nm is enough to mask the event from observation. On the other hand, with a  $J_{1.5}$  of  $10 \text{ cm}^{-3} \text{ s}^{-1}$ , the drop between  $J_{1.5}$  and  $J_3$  should be by a factor of  $10^4$  for the event to become unobservable. The question we want to answer is: If the coagulation sink does not mask a nucleation event at low RH (e.g., 10%), is it possible that such masking would occur solely due to increased coagulation sink if RH increases to a high value (e.g., 90%)? To answer this question, we determine “average” and “extreme” values of particle growth rates and condensation sinks during Hyytiälä nucleation events and calculate (using equation (1)) how much an RH increase from 10 to 90% enhances scavenging of sub-3 nm particles. The average values are taken from *Dal Maso et al.* [2005] who, based on an 8 year dataset of events, found the average GR and CS for dry particle size distribution to be  $3 \text{ nm h}^{-1}$  and  $8.6 \text{ h}^{-1}$ , respectively. To define a “slow growth” case (it is clear that a slow GR will lead to enhanced coagulation scavenging of the clusters between 1.5 and 3 nm) we use a growth rate from the low end of observed values ( $0.5 \text{ nm h}^{-1}$ ) together with the average CS.

[23] Figure 8a shows how  $J_3$  decreases as a function of RH at the average and slow growth cases. In the average case,  $J_3$  at RH = 90% is 0.63 of its value at 10% RH. Thus, it is quite improbable that high RH values could mask nucleation events very efficiently at average conditions. In the slow growth conditions, on the other hand,  $J_3$  drops by a factor of 15, indicating that masking of nucleation events could take place especially if  $J_{1.5}$  is low. Figure 8b reveals that dry coagulation sink alone causes  $J_3$  to be smaller than  $J_{1.5}$  by a factor of about 400. Thus, if  $J_{1.5}$  is  $1 \text{ cm}^{-3} \text{ s}^{-1}$ , the dry sink alone causes  $J_3$  to be  $2.5 \times 10^{-3} \text{ cm}^{-3} \text{ s}^{-1}$ , and the event would be barely observable. The increase of the sink at increased RH would then cause complete masking of the event. Thus, it appears that increased coagulation sink, under certain conditions, may cause the observed suppression of NPF events at high RH values. However, the requirements for that are a low nucleation rate at 1.5 nm, a low GR (in other words, the event needs to be rather weak to begin with), and an appreciable CoagS. Thus, it appears that the increase of the coagulation sink at high RH is at most a secondary reason for the observed suppression of NPF at high RH values.

[24] The following section discusses how much increased CoagS (as well as increased CS and decreased OH formation) may affect observed new particle formation rates.

## 4. Numerical Modeling

### 4.1. Model Description and Setup

[25] The proposed reasons for inhibition of NPF at high RH (i.e., reduced H<sub>2</sub>SO<sub>4</sub> formation rate, increased condensation sink, and increased coagulation sink) were further investigated with an aerosol dynamics model UHMA

[*Korhonen et al.*, 2004]. This box model has previously been used in several studies of NPF [e.g., *Grini et al.*, 2005; *Tunved et al.*, 2006; *Komppula et al.*, 2006; *Sihto et al.*, 2009].

[26] NPF was simulated for 5 h periods at a wide range of conditions representing both clean and polluted environments. In all the simulations, we assumed activation nucleation [*Kulmala et al.*, 2006] together with coagulation and condensation of H<sub>2</sub>SO<sub>4</sub> and a low volatile nonhygroscopic organic compound (saturation concentration of  $10^6 \text{ cm}^{-3}$ ). We calculated explicitly the production of H<sub>2</sub>SO<sub>4</sub> from the SO<sub>2</sub> + OH reaction and its loss by condensation and nucleation, whereas the concentration of the organic vapor was assumed constant. The latter assumption may not be true in atmospheric conditions where the condensable organic vapors are likely formed in photooxidation of plant-emitted VOCs. However, using a constant profile instead of an OH-dependent profile in the simulations does not change the conclusions of this study and is thus assumed here to simplify the interpretation of the model result. For each simulation the concentrations of OH and of SO<sub>2</sub> were fixed (however, they varied between the simulations) and thus the H<sub>2</sub>SO<sub>4</sub> production rate was constant.

[27] Table 1 lists the different values used for SO<sub>2</sub> concentration (affecting the concentration of H<sub>2</sub>SO<sub>4</sub> via the SO<sub>2</sub> + OH reaction), organic vapor concentration (affecting the growth rate of newly formed particles), preexisting particle number concentration (one lognormal mode with geometric mean diameter of 300 nm and a standard deviation of 1.3, affecting the scavenging rate of newly formed particles), and an *A* factor for activation nucleation (nucleation rate at 1 nm  $J = A[\text{H}_2\text{SO}_4]$ ), which affects the formation rate of new particles. The chosen preexisting particle concentrations correspond roughly to CS values 2, 20, and  $200 \text{ h}^{-1}$ . As all the simulations were performed at RH of 10–90%, with 5% increments, we simulated particle formation altogether at 1377 different conditions.

[28] For each of these conditions four model setups were used. For setup 1, the baseline run, OH concentration was set to  $10^6 \text{ cm}^{-3}$  below RH 60% and assumed to decrease linearly at higher RH (reaching  $10^4 \text{ cm}^{-3}$  at RH 100%). This assumption is based on a separate analysis with a chemical model [*Boy et al.*, 2005]. For setup 2, the fixed OH run, OH concentration was kept fixed at  $10^6 \text{ cm}^{-3}$  at all relative humidities. Comparison of this run to the baseline run reveals how much the reduction in the H<sub>2</sub>SO<sub>4</sub> production rate affects the nucleation and NPF rates at high RH. Setup 3, the fixed CS run, was the same as the baseline run except that inside the model’s condensation routine the particle size was always assumed to be the same as that at RH = 10%. The wet size at simulated RH was used for all other modeled processes. Comparison of this run to the baseline run shows how much the increase in the condensation sink due to higher RH affects the H<sub>2</sub>SO<sub>4</sub> concentrations and thus nucleation and NPF rates. Setup 4, the fixed CoagS run, was the same as the baseline run except that inside the coagulation routine the particle size was always assumed to be the same as that at RH = 10%. The wet size at simulated RH was used for all other modeled processes. Comparison of this run to the baseline run shows how much the increase in the coagulation sink due to higher RH affects scavenging of nucleated clusters and thus particle formation rates at 3 nm

**Table 2.** Variables Used in Model Simulations

	OH ( $\text{cm}^{-3}$ )	RH in CS Calculation (%)	RH in CoagS Calculation (%)
Setup 1	$10^4$ – $10^6$	10–90	10–90
Setup 2	fixed at $10^6$	10–90	10–90
Setup 3	$10^4$ – $10^6$	fixed at 10	10–90
Setup 4	$10^4$ – $10^6$	10–90	fixed at 10

( $J_3$ ). For each of these conditions we summarize the four setups used in the model simulations and present these in Table 2. It should be noted that while in reality CS and CoagS values are not independent of each other, in the model they can be fixed separately in order to study their relative importance on the inhibition of nucleation.

#### 4.2. Numerical Modeling Results and Discussion

[29] For each of the simulations we calculated the mean  $\text{H}_2\text{SO}_4$  concentration, nucleation rate (particles formed at 1 nm), and NPF rate (formation rate of 3 nm particles) over the length of the simulation (5 h). It should be noted that although the model assumed that particles form at 1 nm, the conclusions presented below would apply also to particles formed at 1.5 nm.

[30] In Figure 9, we present the ratio of the baseline run mean values to the sensitivity run mean values (model setups 2–4 in the list above). Values below 1 indicate that the mean value in the baseline run is suppressed compared to the sensitivity run. The magnitude of this suppression demonstrates the importance of the RH dependence of OH concentration (setup 2), condensation sink (setup 3) and coagulation scavenging (setup 4) on NPF, respectively. Note that we have left 252 cases out from Figure 9, cases in which the apparent formation rate  $J_3$  in the baseline run was negligibly small (below  $10^{-10} \text{ cm}^{-3} \text{ s}^{-1}$ ).

[31] In accordance with the data analysis performed above, Figure 9 (top left) shows that high RH affects NPF mainly via reduction of OH concentration which leads on average to 59% less  $\text{H}_2\text{SO}_4$  at RH = 90% than at RH < 60%. The lowered  $\text{H}_2\text{SO}_4$  is directly translated to slower cluster formation at 1 nm which together with slower initial growth rate due to  $\text{H}_2\text{SO}_4$  leads to a reduced NPF rate (Figure 9, middle and Figure 9, bottom, respectively). On average the simulated  $J_3$  is reduced by 81% and it is evident that in many of the cases the nucleation event is suppressed totally.

[32] It is important to notice, however, that the RH effect on the condensation sink (Figure 9, middle) is also of some significance. At high RH the increased CS can reduce

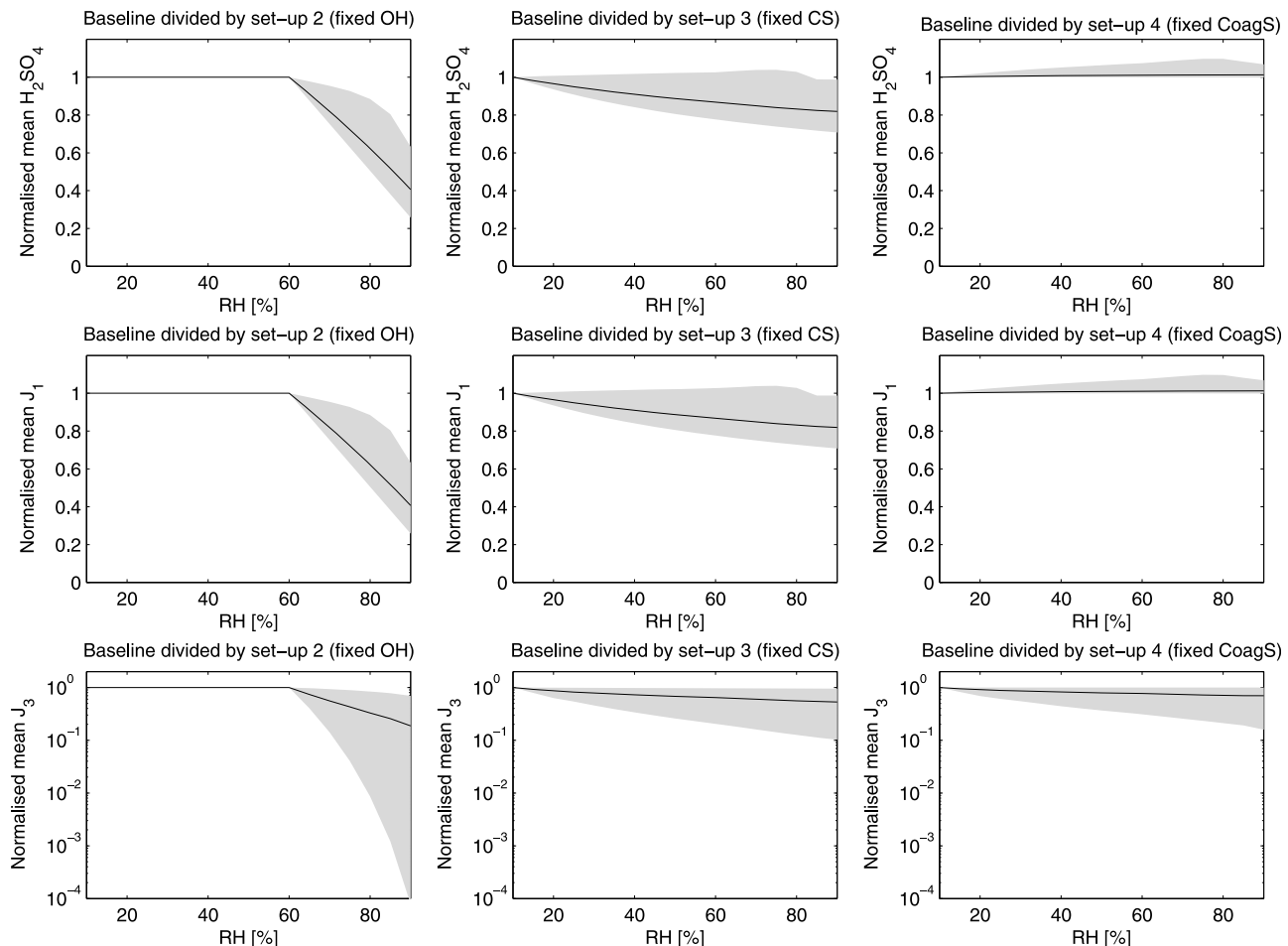


**Figure 9.** Mean (top)  $\text{H}_2\text{SO}_4$  concentration, (middle) nucleation rate ( $J_{1.5}$ ), and (bottom) NPF rate ( $J_3$ ) in the baseline run normalized by the mean values of the sensitivity runs. The shaded area indicates the range of all simulations and the solid curve the mean of the ratios at each relative humidity.

the  $\text{H}_2\text{SO}_4$  by up to 29% compared to dry atmosphere. On average, this effect leads to 47% lower particle formation rate at  $\text{RH} = 90\%$  than it would were the condensation sink independent of RH. The effect of increased coagulation sink (Figure 9, right) on the NPF rate is of the same magnitude as that of increased CS (mean reduction now 30%). As expected, the effect of the coagulation sink on the  $\text{H}_2\text{SO}_4$  and  $J_1$  is of minor importance.

[33] Here, the RH dependence of OH concentration was obtained from a separate analysis with a chemical model. However, some observational studies suggest a weaker RH dependence for the OH concentration. For example, should the dependence arise from cloudiness, *Matthijssen et al.* [1998] observed an  $\sim 90\%$  drop in OH at surface compared to above cloud values. Therefore, we repeated the model runs at all 1377 conditions assuming that the OH concentration drops to  $10^5 \text{ cm}^{-3}$  (and not to  $10^4 \text{ cm}^{-3}$ ) at  $\text{RH} = 100\%$ . This change had only a very minor effect on the ratios presented in Figure 9, which suggests that our conclusions are robust regarding the magnitude of OH concentration drop at high relative humidities.

## 5. Conclusions

[34] There are several reasons why RH has been observed to be anticorrelated with continental NPF: (1) Enhanced coagulation scavenging of sub-3 nm clusters at high RH, (2) diminished solar radiation at high RH leading to diminished gas phase oxidation chemistry, and (3) increased condensation sink of condensable gases due to hygroscopic growth of the preexisting particles. In our study, we used analysis of field measurements (e.g., the QUEST 2003 campaign at Hyytiälä, Finland), theoretical calculations, and box model simulations to examine the role of these factors in detail.

[35] Analysis of the field measurements indicate that sulphuric acid concentrations decreased significantly at RH above 60%. At high RH ( $>80\%$ ) nucleation rates mostly were below  $2 \text{ cm}^{-3} \text{ s}^{-1}$  where the  $\text{H}_2\text{SO}_4$  concentrations were below  $3 \times 10^6 \text{ cm}^{-3}$ . We then tried to separate the factors contributing to  $\text{H}_2\text{SO}_4$  formation and loss rates as a function of RH. Overall, there was no significant RH dependence for the measured  $\text{SO}_2$  concentration although the maximum  $\text{SO}_2$  values decreased slightly with RH during the 2003 QUEST campaign. On the other hand, the UV radiation intensity, which is a proxy for OH concentration, decreased clearly with increasing RH. The interesting finding is that the UV radiation trend was very similar to that of the measured  $\text{H}_2\text{SO}_4$  concentrations, which suggests that the concentration of  $\text{H}_2\text{SO}_4$  at high humidities is controlled by the reduced OH formation rate. It must be noted, however, that the sink term for  $\text{H}_2\text{SO}_4$  increased by a factor of  $\sim 3$  from 30 to 90% RH, and thus may have played some role in the inhibition of nucleation at high RH.

[36] One reason for the anticorrelation between UV radiation and RH is that their diurnal cycles show opposite trends (while radiation intensity peaks at noon, the RH cycle exhibits a minimum at that time). Moreover, a 30 year data set of cloudiness, RH, and global radiation from the Jokioinen observatory ( $\sim 100 \text{ km}$  from Hyytiälä station) showed that low-level cloud cover correlated with ground level RH, and as a result, global solar radiation is anticorrelated with RH.

As a result, RH is anticorrelated with OH production. We therefore conclude that, even though at first glance RH appears to limit NPF, this appearance is due to its anticorrelation with solar radiation. This finding was also supported by the box model simulations.

[37] Further analysis on the role of increased condensation sink and coagulation scavenging was made using theoretical calculations of average and extreme conditions at Hyytiälä as well as box model simulations at a range of clean and polluted conditions. This analysis revealed that while the increased uptake of water by particles does affect the concentration of nucleating vapors and survival of nucleating clusters to some extent, these effects are typically minor in comparison to the reduced OH effect.

[38] **Acknowledgments.** This study is financially supported by the Magnus Ehrnrooth Foundation (grant 2009f19) and the Finnish Cultural Foundation (North Savo Regional Fund). J.N.S. acknowledges funding from the Saastamoinen Foundation and the U.S. Department of Energy (grant DE-FG-02-05ER63997). The National Center for Atmospheric Research is sponsored by the U.S. National Science Foundation. ACCENT and the Academy of Finland (project 107826 and the Center of Excellence program) are acknowledged.

## References

- Aalto, P., et al. (2001), Physical characterization of aerosol particles during nucleation events, *Tellus, Ser. B*, 53, 344–358.
- Alam, A., J. P. Shi, and R. M. Harrison (2003), Observations of new particle formation in urban air, *J. Geophys. Res.*, 108(D3), 4093, doi:10.1029/2001JD001417.
- Birmili, W., and A. Wiedensohler (2000), New particle formation in the continental boundary layer: Meteorological and gas phase parameter influence, *Geophys. Res. Lett.*, 27, 3325–3328.
- Birmili, W., H. Berresheim, C. Plass-Dülmer, T. Elste, S. Gilge, A. Wiedensohler, and U. Uhrner (2003), The Hohenpeissenberg aerosol formation experiment (HAFEX): A long-term study including size-resolved aerosol,  $\text{H}_2\text{SO}_4$ , OH, and monoterpene measurements, *Atmos. Chem. Phys.*, 3, 361–376.
- Bonn, B., and G. K. Moortgat (2003), Sesquiterpene ozonolysis: Origin of atmospheric new particle formation from biogenic hydrocarbons, *Geophys. Res. Lett.*, 30(11), 1585, doi:10.1029/2003GL017000.
- Bonn, B., G. Schuster, and G. K. Moortgat (2002), Influence of water vapor on the process of new particle formation during monoterpene ozonolysis, *J. Phys. Chem. A*, 106, 2869–2881.
- Boy, M., and M. Kulmala (2002), Nucleation events in the continental boundary layer: Influence of physical and meteorological parameters, *Atmos. Chem. Phys.*, 2, 1–16.
- Boy, M., et al. (2005), Sulphuric acid closure and contribution to nucleation mode particle growth, *Atmos. Chem. Phys.*, 5, 863–878.
- Clarke, A. D., J. Varner, F. Eisele, R. Mauldin, D. Tanner, and M. Litchy (1998), Particle production in the remote marine atmosphere: Cloud outflow and subsidence during ACE 1, *J. Geophys. Res.*, 103, 16,397–16,409, doi:10.1029/97JD02987.
- Dal Maso, M., M. Kulmala, I. Riipinen, R. Wagner, T. Hussein, P. P. Aalto, and K. E. J. Lehtinen (2005), Formation and growth of fresh atmospheric aerosols: Eight years of aerosol size distribution data from SMEAR II, Hyytiälä, Finland, *Boreal Environ. Res.*, 10, 323–336.
- Grini, A., H. Korhonen, K. E. J. Lehtinen, I. Isaksen, and M. Kulmala (2005), A combined photochemistry/aerosol dynamics model: Model development and a study of new particle formation, *Boreal Environ. Res.*, 10, 525–541.
- Hamed, A., et al. (2007), Nucleation and growth of new particles in Po Valley, Italy, *Atmos. Chem. Phys.*, 7, 355–376.
- Hämmeri, K., M. Väkevä, H.-C. Hansson, and A. Laaksonen (2000), Hygroscopic growth of ultrafine ammonium sulphate aerosol measured using an ultrafine tandem differential mobility analyzer, *J. Geophys. Res.*, 105, 22,231–22,242, doi:10.1029/2000JD900220.
- Hanke, M., J. Uecker, T. Reiner, and F. Arnold (2002), Atmospheric proxy radicals: ROXMAS, a new mass-spectrometric methodology for speciated measurements of  $\text{HO}_2$  and sigma  $\text{RO}_2$  and first results, *Int. J. Mass Spectrom.*, 213, 91–99.
- Hari, P., and M. Kulmala (2005), Station for measuring ecosystem-atmosphere relations (SMEAR II), *Boreal Environ. Res.*, 10, 315–322.

- Hegg, D. A., L. F. Radke, and P. V. Hobbs (1990), Particle production associated with marine clouds, *J. Geophys. Res.*, *95*, 13,917–13,926.
- Hyvönen, S., et al. (2005), A look at aerosol formation using data mining techniques, *Atmos. Chem. Phys.*, *5*, 3345–3356.
- Iida, K., M. R. Stolzenburg, and P. H. McMurry (2009), Effect of working fluid on sub-2 nm particle detection with a laminar flow ultrafine condensation particle counter, *Aerosol Sci. Technol.*, *43*, 81–96.
- Jaatinen, A., et al. (2009), A comparison of new particle formation events at three different sites in the European boundary layer, *Boreal Environ. Res.*, *14*, 481–498.
- Jeong, C. H., P. K. Hopke, D. Chalupa, and M. Utell (2004), Characteristics of nucleation and growth events of ultrafine particles measured in Rochester, N.Y., *Environ. Sci. Technol.*, *38*, 1933–1940.
- Keil, A., M. Wendisch, and E. Brüggemann (2001), Measured profiles of aerosol particle absorption and its influence on clear-sky solar radiative forcing, *J. Geophys. Res.*, *106*, 1237–1247.
- Kerminen, V.-M., and M. Kulmala (2002), Analytical formulae connecting the “real” and the “apparent” nucleation rate and the nuclei number concentration for atmospheric nucleation events, *J. Aerosol. Sci.*, *33*, 609–622.
- Komppula, M., M. Dal Maso, H. Lihavainen, P. P. Aalto, M. Kulmala, and Y. Viisanen (2003), Comparison of new particle formation events at two locations in northern Finland, *Boreal Environ. Res.*, *8*, 395–404.
- Komppula, M., S.-L. Sihto, H. Korhonen, H. Lihavainen, V.-M. Kerminen, M. Kulmala, and Y. Viisanen (2006), New particle formation in air mass transported between two measurement sites in northern Finland, *Atmos. Chem. Phys.*, *6*, 2811–2825.
- Korhonen, H., K. E. J. Lehtinen, and M. Kulmala (2004), Multicomponent aerosol dynamics model UHMA: Model development and validation, *Atmos. Chem. Phys.*, *4*, 757–771.
- Kulmala, M. (2003), How particles nucleate and grow, *Science*, *302*, 1000–1001.
- Kulmala, M., M. Dal Maso, J. M. Mäkelä, L. Pirjola, M. Väkevä, P. Aalto, P. Mikkulainen, K. Hämeri, and C. D. O’Dowd (2001), On the formation, growth, and composition of nucleation mode particles, *Tellus, Ser. B*, *53*, 479–490.
- Kulmala, M., H. Vehkamäki, T. Petäjä, M. Dal Maso, A. Lauri, V.-M. Kerminen, W. Birmili, and P. H. McMurry (2004a), Formation and growth rates of ultrafine atmospheric particles: A review of observations, *J. Aerosol Sci.*, *35*, 143–176.
- Kulmala, M., V.-M. Kerminen, T. Anttila, A. Laaksonen, and C. D. O’Dowd (2004b), Organic aerosol formation via sulphate cluster activation, *J. Geophys. Res.*, *109*, D04205, doi:10.1029/2003JD003961.
- Kulmala, M., K. E. J. Lehtinen, and A. Laaksonen (2006), Cluster activation theory as an explanation of the linear dependence between formation rate of 3 nm particles and sulphuric acid concentration, *Atmos. Chem. Phys.*, *6*, 787–793.
- Kulmala, M., et al. (2007), Toward direct measurement of atmospheric nucleation, *Science*, *318*, 89–92.
- Laakso, L., T. Petäjä, K. E. J. Lehtinen, M. Kulmala, J. Paatero, U. Hörrak, H. Tammet, and J. Joutsensaari (2004), Ion production rate in a boreal forest based on ion, particle, and radiation measurements, *Atmos. Chem. Phys.*, *4*, 1933–1943.
- Laaksonen, A., et al. (2008), The role of VOC oxidation products in continental new particle formation, *Atmos. Chem. Phys.*, *8*, 2657–2665.
- Lehtinen, K. E. J., M. Dal Maso, M. Kulmala, and V. M. Kerminen (2007), Estimating nucleation rates from apparent particle formation rates and vice versa: Revised formulation of the Kerminen-Kulmala equation, *J. Aerosol Sci.*, *38*, 988–994.
- Lyubovtseva, Y. S., L. Sogacheva, M. Dal Maso, B. Bonn, P. Keronen, and M. Kulmala (2005), Seasonal variations of trace gases, meteorological parameters, and formation of aerosols in boreal forests, *Boreal Environ. Res.*, *10*, 493–510.
- Matthijsen, J., K. Suhre, R. Rosset, F. L. Eisele, R. L. Mauldin III, and D. J. Tanner (1998), Photodissociation and UV radiative transfer in a cloudy atmosphere: Modeling and measurements, *J. Geophys. Res.*, *103*, 16,665–16,676, doi:10.1029/97JD02989.
- McMurry, P. H., and S. K. Friedlander (1979), New particle formation in the presence of an aerosol, *Atmos. Environ.*, *13*, 1635–1651.
- Mikkonen, S., K. E. J. Lehtinen, A. Hamed, J. Joutsensaari, M. C. Facchini, and A. Laaksonen (2006), Using discriminant analysis as a nucleation event classification method, *Atmos. Chem. Phys.*, *6*, 8485–8510.
- Petäjä, T., R. L. Mauldin, E. Kosciuch, J. McGrath, T. Nieminen, P. Paasonen, M. Boy, A. Adamov, T. Kotiaho, and M. Kulmala (2009), Sulphuric acid and OH concentrations in a boreal forest site, *Atmos. Chem. Phys.*, *9*, 7435–7448.
- Pirjola, L., A. Laaksonen, P. Aalto, and M. Kulmala (1998), Sulfate aerosol formation in the Arctic boundary layer, *J. Geophys. Res.*, *103*, 8309–8322.
- Rohrer, F., and H. Berresheim (2006), Strong correlation between levels of tropospheric hydroxyl radicals and solar ultraviolet radiation, *Nature*, *442*, 184–187.
- Sihto, S.-L., et al. (2006), Atmospheric sulphuric acid and aerosol formation: implications from atmospheric measurements for nucleation and early growth mechanisms, *Atmos. Chem. Phys.*, *6*, 4079–4091.
- Sihto, S.-L., H. Vuollekoski, J. Leppä, I. Riipinen, V.-M. Kerminen, H. Korhonen, K. E. J. Lehtinen, M. Boy, and M. Kulmala (2009), Aerosol dynamics simulations on the connection of sulphuric acid and new particle formation, *Atmos. Chem. Phys.*, *9*, 2933–2947.
- Sipilä, M., et al. (2010), The role of sulphuric acid in atmospheric nucleation, *Science*, *327*, 1234–1246.
- Stanier, C. O., A. Y. Khlystov, and S. N. Pandis (2004), Nucleation events during the Pittsburgh air quality study: Description and relation to key meteorological, gas phase, and aerosol parameters, *Aerosol Sci. Technol.*, *38*, 253–264.
- Tunved, P., H. Korhonen, J. Ström, H.-C. Hansson, K. E. J. Lehtinen, and M. Kulmala (2006), Is nucleation capable of explaining observed aerosol integral number during southerly transport over Scandinavia?, *Tellus, Ser. B*, *58*, 129–140.
- Vaattovaara, P., et al. (2009), The evolution of nucleation and Aitken-mode particle compositions in a boreal forest environment during clean and pollution-affected new-particle formation events, *Boreal Environ. Res.*, *14*, 662–682.
- Weber, R. J., J. J. Marti, P. H. McMurry, F. L. Eisele, D. J. Tanner, and A. Jefferson (1997), Measurements of new particle formation and ultrafine particle growth rates at a clean continental site, *J. Geophys. Res.*, *102*, 4375–4385.
- Weber, R. J., P. H. McMurry, R. L. Mauldin, D. J. Tanner, F. L. Eisele, A. D. Clarke, and V. N. Kapustin (1999), New particle formation in the remote troposphere: A comparison of observations at various sites, *Geophys. Res. Lett.*, *26*, 307–310.
- Woo, K. S., D. R. Chen, D. Y. H. Pui, and P. H. McMurry (2001), Measurement of Atlanta aerosol size distributions: Observations of ultrafine particle events, *Aerosol Sci. Technol.*, *34*, 75–87.

F. Arnold, Atmospheric Physics Division, Max-Planck Institute for Nuclear Physics, PO Box 103980, D-69029, Heidelberg, Germany.

A. Hamed, J. Joutsensaari, A. Laaksonen, K. E. J. Lehtinen, and J. N. Smith, Department of Physics and Mathematics, University of Eastern Finland, Kuopio Campus, PO Box 70211, FI-70211, Kuopio, Finland. (amar.hamed@uef.fi)

H. Järvinen, Finnish Meteorological Institute, PO Box 503, FI-00101, Helsinki, Finland.

H. Korhonen, Finnish Meteorological Institute, PO Box 1627, FI-70210 Kuopio, Finland.

M. Kulmala, T. Nieminen, T. Petäjä, and S.-L. Sihto, Department of Physics, University of Helsinki, PO Box 64, FI-00014, Helsinki, Finland.